AFRL-ML-WP-TR-2003-4022

NONDESTRUCTIVE EVALUATION (NDE) TECHNOLOGY INITIATIVES

Delivery Order 0021: Application of an Electrochemical Fatigue Sensor (EFS) Borescope System for Military Turbine Engine Assessment

R. Krupa
R. Tillinghast
T. Root

Materials Technologies, Inc.
DBA Tensiodyne Scientific Corporation
1161 San Vicente Blvd, Suite 707
Los Angeles, CA 90049

Optim Incorporated
64 Technology Park Road
Sturbridge, MA 01566-1262

OCTOBER 2002

Final Report for 01 November 2000 – 31 October 2002

MATERIALS AND MANUFACTURING DIRECTORATE
AIR FORCE RESEARCH LABORATORY
AIR FORCE MATERIEL COMMAND
WRIGHT-PATTERSON AIR FORCE BASE, OH 45433-7750

NOTICE

THIS TECHNICAL REPORT HAS BEEN REVIEWED AND IS APPROVED FOR PUBLICATION.

Juan G. Calzada

JUAN G. CALZADA, Project Engineer
Nondestructive Evaluations Branch
Metals, Ceramics & NDE Division

James C Malas

JAMES C. MALAS, Chief
Nondestructive Evaluations Branch
Metals, Ceramics & NDE Division

GERALD J. PETRAK, Assistant Chief
Metals, Ceramics & NDE Division
Materials & Manufacturing Directorate

REPORT DOCUMENTATION PAGE

Form Approved
OMB No. 0704-0188

1. REPORT DATE *(DD-MM-YY)*	2. REPORT TYPE	3. DATES COVERED *(From - To)*
October 2002	Final	11/01/2000 – 10/31/2002

4. TITLE AND SUBTITLE
NONDESTRUCTIVE EVALUATION (NDE) TECHNOLOGY INITIATIVES
Delivery Order 0021: Application of an Electrochemical Fatigue Sensor (EFS) Borescope System for Military Turbine Engine Assessment

5a. CONTRACT NUMBER F33615-97-D-5271
5b. GRANT NUMBER
5c. PROGRAM ELEMENT NUMBER 62102F

6. AUTHOR(S)
R. Krupa
R. Tillinghast
T. Root

5d. PROJECT NUMBER 4349
5e. TASK NUMBER 40
5f. WORK UNIT NUMBER 01

7. PERFORMING ORGANIZATION NAME(S) AND ADDRESS(ES)
Materials Technologies, Inc.
DBA Tensiodyne Scientific Corporation
1161 San Vicente Blvd, Suite 707
Los Angeles, CA 90049

Optim Incorporated
64 Technology Park Road
Sturbridge, Ma 01566-1262

8. PERFORMING ORGANIZATION REPORT NUMBER
ES0408

9. SPONSORING/MONITORING AGENCY NAME(S) AND ADDRESS(ES)
Materials and Manufacturing Directorate
Air Force Research Laboratory
Air Force Materiel Command
Wright-Patterson AFB, OH 45433-7750

10. SPONSORING/MONITORING AGENCY ACRONYM(S)
AFRL/MLLP

11. SPONSORING/MONITORING AGENCY REPORT NUMBER(S)
AFRL-ML-WP-TR-2003-4022

12. DISTRIBUTION/AVAILABILITY STATEMENT
Approved for public release; distribution is unlimited.

13. SUPPLEMENTARY NOTES
Report contains color.

14. ABSTRACT
The objective for this project was to improve the United States Air Force's capability to perform fatigue assessment of military aircraft engines through the application of four nondestructive technologies: eddy current inspection, ultrasonic inspection, visual inspection, and the electrochemical fatigue sensor (EFS).

EFS is a relatively new technology; the other three inspection methodologies are well established and widely accepted means of component inspection. A 6-mm-diameter inspection borescope, capable of delivering ultrasonic, eddy current, and EFS probes, along with video imaging, to fatigue critical locations within an engine has been developed. The 3-mm ID working channel within the borescope permits the delivery of the three probes. An intuitive user interface employing a mechanical joystick is used to articulate the borescope in all directions over a hemisphere of operation.

While the EFS probe could be delivered, along with the electrolyte gel, through the borescope, the technology is not currently available to stress the turbine blades with enough force and control to permit EFS signal generation within the confines of an engine. Work is necessary in producing the loading mechanism within an engine, and on improving engine access on future designs.

15. SUBJECT TERMS
Electrochemical fatigue sensor, turbine engine, fiberscope, borescope, eddy current, ultrasonic

16. SECURITY CLASSIFICATION OF: a. REPORT	b. ABSTRACT	c. THIS PAGE	17. LIMITATION OF ABSTRACT:	18. NUMBER OF PAGES	19a. NAME OF RESPONSIBLE PERSON (Monitor)
Unclassified	Unclassified	Unclassified	SAR	38	Juan G. Calzada **19b. TELEPHONE NUMBER** *(Include Area Code)* (937) 255-1605

Standard Form 298 (Rev. 8-98)
Prescribed by ANSI Std. Z39-18

TABLE OF CONTENTS

LIST OF FIGURES

Figure Page

SUMMARY

The objective for this project was to improve the United States Air Force's capability to perform fatigue assessment of military aircraft engines through the application of four nondestructive technologies: eddy current inspection, ultrasonic inspection, visual inspection, and the electrochemical fatigue sensor.

While the electrochemical fatigue sensor (EFS) is a relatively new technology, the other three inspection methodologies are well established and widely accepted means of component inspection. A 6mm diameter inspection borescope, capable of delivering ultrasonic, eddy current, and EFS probes, along with video imaging, to fatigue critical locations within an engine has been developed. The 3mm ID working channel within the borescope permits the delivery of the three probes. An intuitive user interface employing a mechanical joystick is used to articulate the borescope in all directions over a hemisphere of operation.

While the EFS probe could be delivered, along with the electrolyte gel, through the borescope, the technology is not currently available to stress the turbine blades with enough force and control to permit EFS signal generation within the confines of an engine. Work is necessary in producing the loading mechanism within an engine, and on improving engine access on future designs.

1.0 Project Objectives

The overall objective for this project is to improve the United Sates Air Force's capability to perform fatigue assessment of military aircraft engines through the application of four nondestructive technologies:

- Eddy Current Inspection
- Ultrasonic Inspection
- Visual Inspection Through a Flexible Borescope
- Electrochemical Fatigue Sensor

While the electrochemical fatigue sensor (EFS) is a relatively new technology, the other three inspection methodologies are well established and widely accepted means of component inspection. However, this is the first instrument that permits the delivery of eddy current (EC) and ultrasonic (UT) transducers, under visual guidance, to the internal components of an aircraft engine through standard borescope access ports in the engine's housing. The EFS sensor is also capable of being delivered to fatigue critical locations within an engine. However, technological advances in force generators are not currently capable of producing the load required to generate EFS signals within the tight space constraints of today's aircraft engines.

2.0 Electrochemical Fatigue Sensor System

A bench top load generation system was developed in order to evaluate the mechanism required to produce an EFS signal, and to verify that the data collection scheme produced the required signal-to-noise ratio necessary for measuring an EFS signal.

2.1 EFS Electrolyte Gel

The electrolyte gel used for this work was prepared by making a concentrated solution of the water-soluble salts that is later added to a gel forming suspension. For the preparation of 1L of the electrolyte gel, the following procedure was employed:

1. Weigh out 16.6g Boric Acid (CAS#10043-35-3), 28.6g Hydrated Sodium Borate (CAS#1303-96-4), and 1.5g Hydrated Sodium Molybdate (CAS#10102-40-6).
2. Dissolve the above salts in 200mL deionized water brought to a temperature of approximately 60°C using a double boiler. At room temperature, the salts do not readily dissolve completely at this concentration.
3. Weigh out 18.75g Laponite RD and 18.75g Laponite RDS (Southern Clay Products, Inc., 1212 Church St., Gonzales, TX 78629, 830-672-2891).
4. In a 1500mL glass beaker, add 800mL of deionized water. Stir the water with a propeller blade at 600-700 RPM. To the stirred water, slowly add the Laponite powders at a rate of approximately 1g/minute, taking care not to add more than 200mg at a time to the water mixture. If more than this is added at once, the clay powder will form clumps and will not properly disperse in the liquid. After all the Laponite powder is added to the beaker, continue stirring the suspension for approximately 30 additional minutes.
5. Add the 200mL of electrolyte concentrate to the stirred clay suspension slowly over a period of approximately 5 minutes. After all the electrolyte solution has been added, continue stirring for an additional 30 minutes.
6. Immediately after this 30-minute stirring period, pour the mixture into a 1L Nalgene bottle and tightly secure the top of the bottle. The mixture is thixotropic, and will become gelatinous in a few minutes.
7. To use the gel, shake the Nalgene bottle vigorously for 60 seconds. This will reduce the viscosity of the gel to the point where it can be poured. Upon storage of the gel, a small volume of water will accumulate on the surface of the gel material. Be sure to mix the mixture prior to taking a portion of the gel from the container in order to maintain the proper concentration of the aliquot taken, and the remaining gel.

For delivery of the gel through the borescope, a 15cc syringe is used to sample a portion of the recently mixed gel. The gel can be pushed down a length of 2mm OD tubing to the distal end of the borescope within a few minutes of loading the syringe. Once the gel has left the tubing (onto the sample), its viscosity will increase rapidly. If the gel is not used within a few minutes of loading the syringe, shake the syringe to mix the gel until a significant decrease in viscosity is observed (approximately 30-60 seconds). The gel is spread over the area that is to be interrogated by the EFS

electronics. Large areas, greater than one square inch, can be interrogated in a single EFS measurement. However, while spreading the gel over a large area increases the speed of analysis, it sacrifices spatial resolution. An EFS signal indicative of a crack cannot be pinpointed more accurately than the area of the area covered by the electrolyte gel.

At the proximal end of the tubing is a box containing a “T” tube with one side arm connected to the gel delivery syringe, and the other connected to a BNC connector mounted on the side of the box. Running the length of the 2mm tubing, and exiting the tube in a “T” connection, is a shielded copper wire attached to a small section of 2mm OD stainless steel tubing at the distal end of the probe. Over the stainless steel tubing, and overlapping the 2mm tubing slightly, is a small piece of heat shrink material. The heat shrink extends slightly beyond the stainless electrode so that the tip of the probe can be in direct contact with the gel, and even the grounded sample, without the electrode making direct contact with the sample. Once the tip of the probe is placed into the recently deposited gel, the stainless tubing acts as the EFS electrode.

The EFS electrode is constructed of a 10mm x 2mm OD stainless steel tube soldered to the shielded cable running the length of the 2mm OD PEBAX tubing. Stainless steel by itself produces a very poor electrode for the conduction of the small electrochemical current produced. Therefore, the stainless steel surface is electroplated with catalytic platinum black. This is done by immersing the steel in a solution of approximately 3.5% Chloroplatinic Acid (CAS# 16941-12-1) and 0.5% Lead Acetate (CAS# 6080-56-4), and applying a current density of approximately 30mA/cm^2 through the solution. This was accomplished by connecting a 9V battery to the stainless steel tubing (+) and a platinum wire (-) through a 477Ω current limiting resistor. Current was allowed to flow for a period of approximately 5 minutes, after which time the stainless tubing was rinsed in deionized water. The appearance of the stainless at this point is a dull black due to the high surface area of the platinum coating.

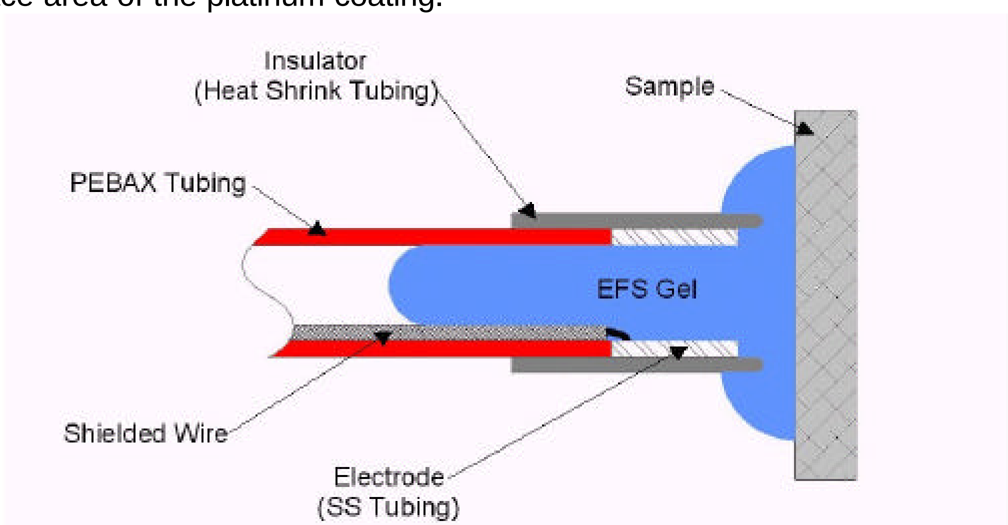

Figure 1. EFS Probe

2.2 Load Generation

The bench top load generator system consisted of a means to hold a test sample, and a mount for the load generator. A BEI KIMCO Linear Actuator, Model #LA24-200-000A, was driven with the sinusoidal output current form a KEPCO Op Amp, Model #BOP-20-10M. The sine wave reference signal was generated by a lock-in amplifier, and was amplified by the op-amp to produce the desired output force at the linear actuator. For the bench top actuator, the sinusoidal force on the sample had a minimum of 4 pounds and a maximum of 15 pounds; or an 11-pound AC force with a 9.5-pound DC component. This corresponded to an 18ksi sinusoidal load on the sample, with a DC offset of 16ksi. The offset ensured that the test piece was always under a load so that the linear actuator remained in contact with the sample at all times. This resulted in a pure sinusoidal load applied to the test sample. If the actuator were permitted to retract completely from the test sample, the sinusoidal wave pressure would be interrupted, and the resulting signal would be a complex function rather than a simple sine wave. The load generator action on the sample is schematically shown in Figure 2.

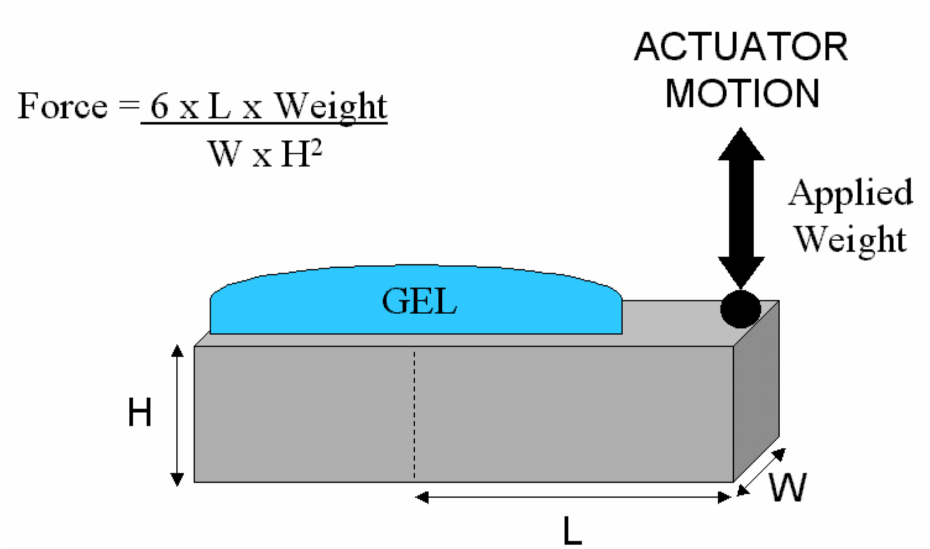

Figure 2. Schematic Representation of Load Actuator on Test Sample.

With this system, we were capable of producing up to 40ksi load on the sample, which compared favorable with previous studies in which EFS signals were generated with 10-30ksi. Figure 3 is a photograph of the system in operation.

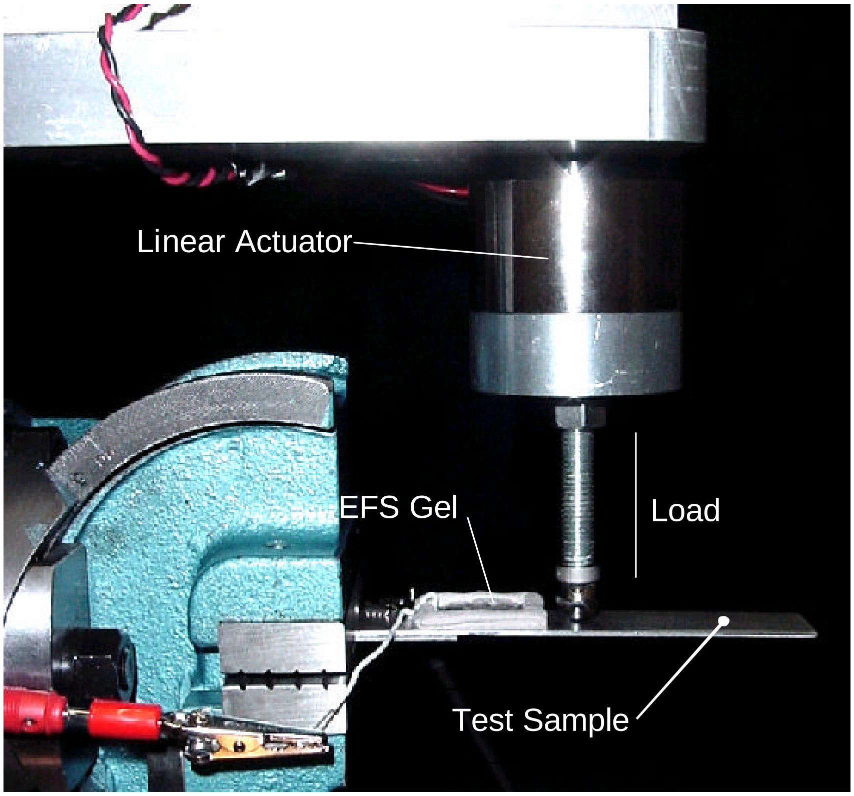

Figure 3. Photograph of Actuator and Sample.

While the application of the load required to produce an EFS signal on the bench top sample was accomplished with readily available components, generating a load of 10 pounds or more within the confines of an engine was more challenging.

In order to produce the desired EFS signal, a force of 8-10 pounds is required to produce 0.1% strain at the turbine blade root, assuming the load is applied to the tip of the blade. This requires the displacement at the blade tip reach 0.5-1mm. In other words, the actuator must have a 0.5-1mm displacement capability. In addition to the sinusoidal displacement required, a static displacement of 1-4mm is required because of the movement of the blade within the engine when it is at ambient temperature (thermal expansion holds the blade firmly in place when the engine is in operation and at an elevated temperature). The additional requirements for the actuator are it must fit through a 6.3mm diameter borescope access hole in the engine, and it must operate at a frequency above 1Hz, preferably above 5Hz. We investigated several different actuators for this application.

A stack of piezoelectric transducers (PZT) can generate forces up to approximately 200 pounds, and at frequencies up to approximately 5KHz. These ceramic materials can be quite small in diameter, on the order of 5-6mm, but the displacement for each individual transducer is only a fraction of what is required to produce the displacement required for this application. Even a stack of transducers on the order of 2" long would only produce

a displacement of a few thousands of an inch. This is much less than is required for the current application.

Electronic solenoids are capable of the required displacement, and capable of an offset displacement able to rigidly hold the blade in place during the measurement. The frequency response of this type of actuator is adequate for the application, with frequency responses in the tens of Hz quite common. However, under 10mm in diameter, electronics solenoids do not have the force generating capability necessary to generate the required 8-10 pounds of force on the blade.

There are a variety of ultrasonic motion devices, loosely classified as ultrasonic motors that are capable of meeting the displacement and force requirements for this application. However, the size of this class of devices is quite large (>10mm).

Magnetorestrictive material, such as terfenol, suffers from its inability to produce the required displacement, with most materials having motion ranges in the sub-millimeter range. It is also unclear at present if material is available in a small package size that is capable of generating the force required.

Liquid pressure in the form of a piston has the potential to generate the required force and displacement. However, the frequency response is quite low, and the size above the necessary 6mm maximum.

Lastly, we investigated the original concept of wedging a washer between the blade tip and its seal. The use of an engine turning tool could then be utilized to rotate the engine against the resistance of this wedge, producing the required force at the blade root. This approach could quite possibly generate the force required for EFS signal generation, but would be time consuming in its implementation in actual usage (requiring the insertion and retraction of two borescopes and washer for each blade to be interrogated). Additionally, the engine turning tool and engine transmissions we investigated had a very large amount of radial play, as much as several degrees, and a large amount of backlash. Because of the play between the input device (engine turning tool motor) and the resulting force on the individual turbine blade, the irreproducibility of the resultant force would undoubtedly be the limiting noise component in the system.

2.3 EFS Data Collection

In our experimentation, the part under interrogation was at ground potential, and a wire placed into the EFS gel, but not in contact with the sample, was connected to the Counter and Reference terminals on the AMEL 2059 Potentiostat. The Potentiostat was operated at +0.455V with the Working terminal connected to the sample and ground. The output of the potentiostat was filtered by a Stanford Research Systems Dual Channel low-pass filter. The potentiostat output was fed into both input channels of the low-pass filter; each channel cutoff frequency was adjusted for each of the signal frequencies of interest: channel 1 had a cutoff frequency of 6Hz and was used to filter the fundamental 5Hz signal, while channel 2 had a cutoff frequency of 12 Hz and was

used to filter the 2f (plastic) signal occurring at 10Hz. Each of the low-pass filter outputs, one at 5Hz and one at 10Hz, was sent to the input of a Stanford Research Systems SR830 Lock-in amplifier where both the phase and magnitude of the EFS signal could be obtained. The internal oscillator of the 5 Hz lock-in was used as the system's trigger, producing a 1V sine wave employed to drive the KEPCO op-amp and subsequently the linear actuator, as well as providing the reference signal for the 10Hz lock-in that was operated in 2f mode.

Analog outputs from the lock-in amplifiers, as well as the 5Hz reference signal, were sent to a BNC-to-ribbon cable box, and then to a Computer Boards PCI-DAS 1602/16 16-bit, 16 channel A/D residing in a desktop computer. Data from the A/D could be collected and directly imported into an Excel spreadsheet for further analysis and plotting using software compatible with the Computer Boards A/D converter (Computer Boards DAS Wizard software). The entire EFS bench top system is depicted schematically in Figure 4.

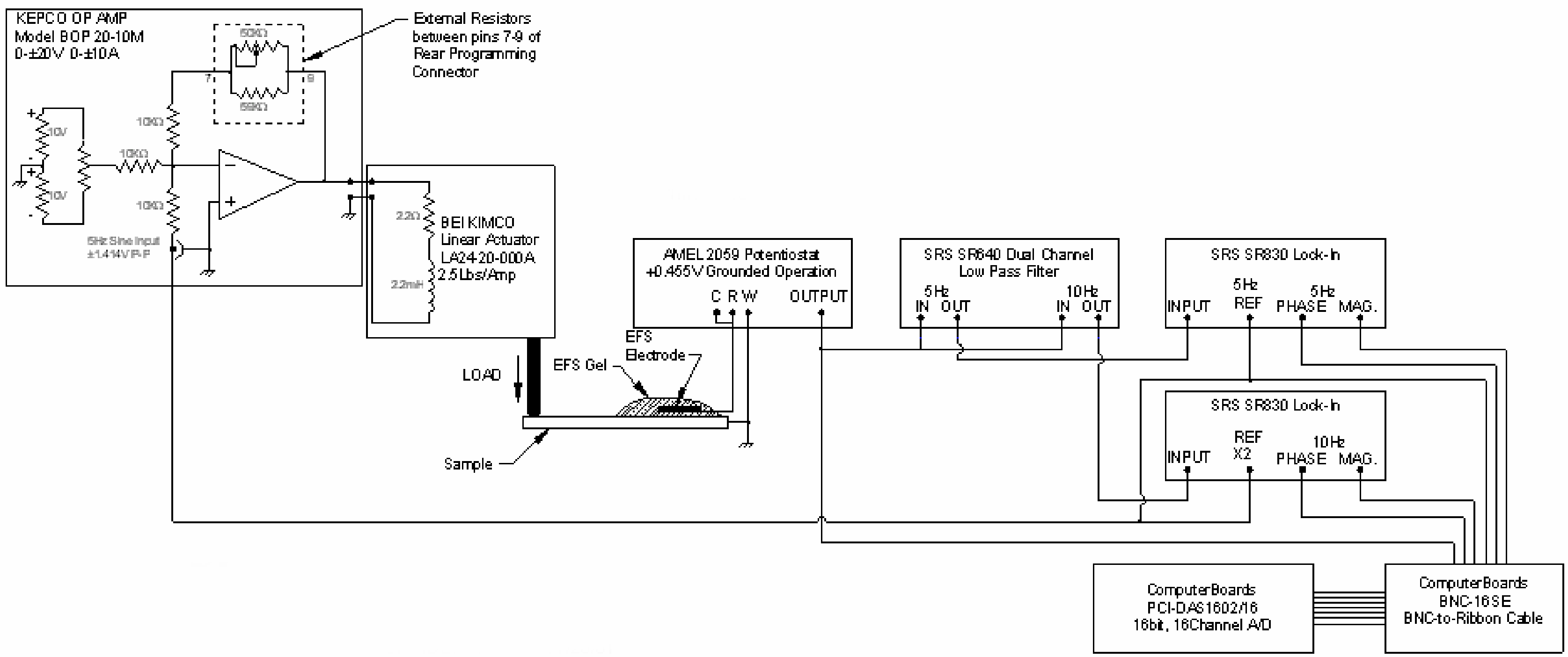

Figure 4. EFS Bench Top Block Diagram

2.4 EFS SIGNAL

As mentioned previously, the application of a sinusoidal load to the sample produces a pure sinusoidal EFS signal. While this signal can have higher harmonic components due to cracks, the signal is a simple waveform that can be easily filtered by conventional analog electronics. This avoids the rapid collection of thousands of noisy data points that must be digitally filtered and manipulated by software.

Raw EFS signal output from the potentiostat is in the micro amp range and contains a large amount of high frequency noise. In fact, typical potentiostat outputs are shown in Figure 5. The blue trace is the unfiltered EFS signal from the potentiostat, composed of

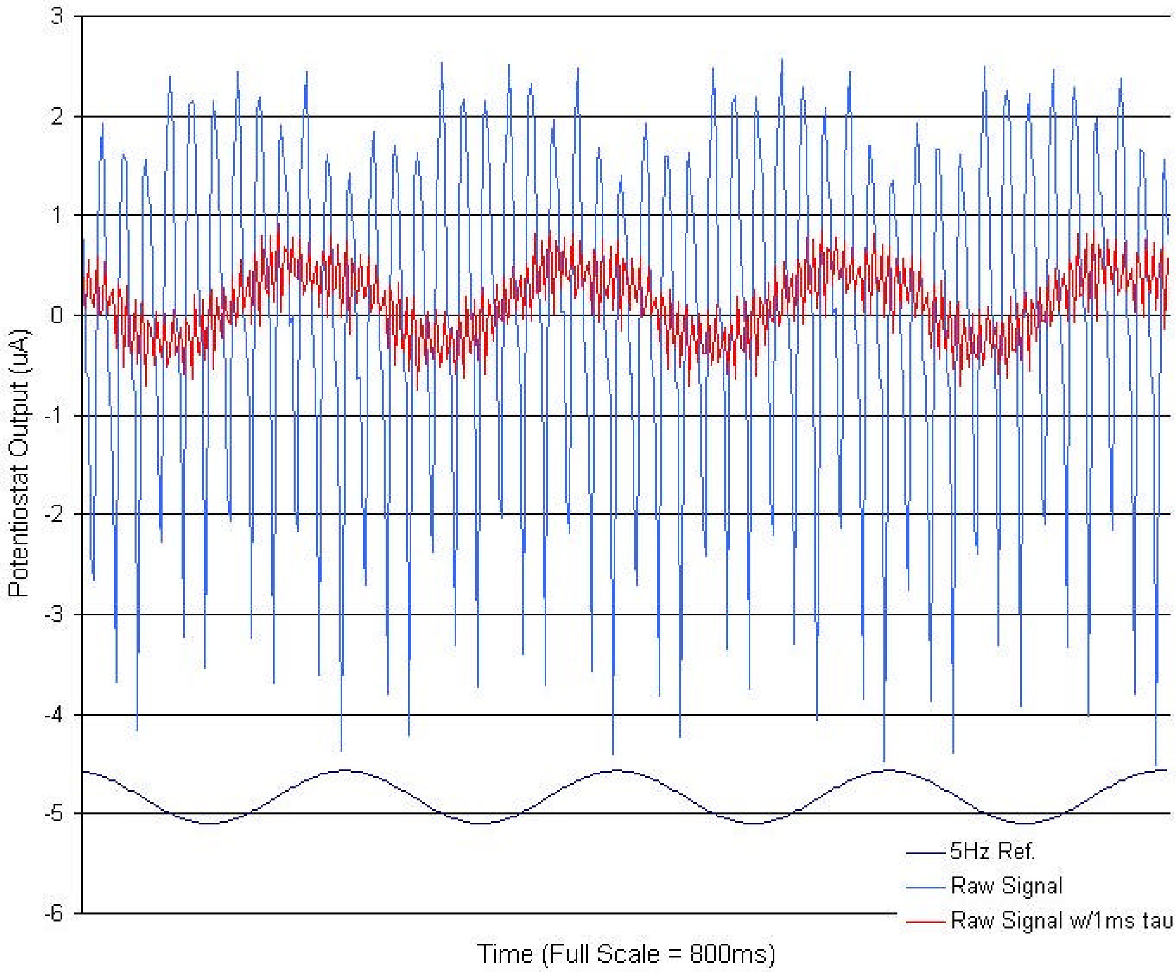

Figure 5. Potentiostat Output

primarily a 60Hz component and a small 120Hz component modulated at 5Hz – the modulation frequency of the applied load. In this situation, the 5Hz EFS signal is barely discernable from the noise, and exhibits a signal-to-noise ratio of approximately 1. Switching on the potentiostat’s 1KHz low pass filter, which also includes a 60Hz notch filter, dramatically reduces the amount of 60Hz flicker, and improves the Signal-to-Noise

Ratio (S/N) to approximately 6. However, the 120Hz flicker and shot noise remain, even after selecting the potentiostat's output filter. While the shot noise could be reduced by integrating the signal longer (increasing the system's time constant), the 120Hz flicker cannot be significantly reduced by collecting more data. Therefore, digitally collecting this data, even over long periods of time, could somewhat reduce the line frequency and its harmonics noise contribution, but it could never eliminate it. Analog signal processing employing active filters, on the other hand, can dramatically reduce both the line frequency-generated flicker noise as well as the shot noise, dramatically improving the S/N over digital signal processing. This is important if this technique is to be used in the field because improving the S/N relates to the amount of time required to perform an analysis (the higher the S/N, the shorter the required integration time).

To ensure that we were indeed viewing actual EFS signals, rather than noise or coupling of the reference signal into the EFS electronics, data was collected in several different modes. This is depicted in Figure 6. With the Potentiostat Signal lead grounded through a 200Ω resister (blue trace), a small amount of signal is being detected by the potentiostat. Lowering the impedance to ground would have reduced or eliminated this, showing that there appears to be no induced signal through the electrode while in the EFS gel and in contact with the sample. The violet trace is the signal generated when the potentiostat signal lead is uncoupled from the gel and left floating in the air. This signal is probably a coupling of the induction coil driving the load actuator to the unshielded signal wire that is in close proximity. The green trace represents the signal generated when the entire system is configured to collect data, except the potentiostat's voltage is turned off. This is the background pick up of the EFS signal wire in the gel, again probably being influenced by the induction coil's radiation.

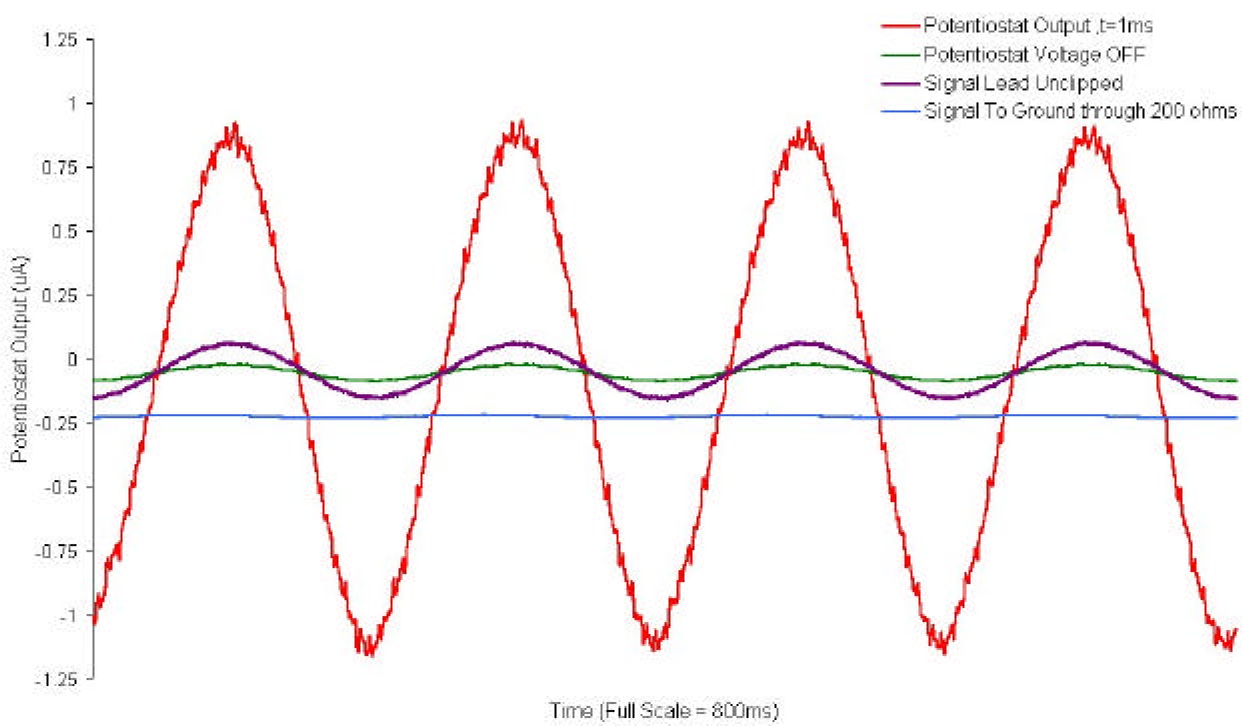

Figure 6. EFS Noise

The single frequency, 5Hz sinusoidal signal is indicative of an unstressed sample. However, when the sample begins to show signs of fatigue and develop cracks, the simple sinusoidal develops a higher frequency component at twice the reference signal. This is demonstrated in Figure 7 in which a 316 stainless steel sample was stressed for several hours, during which time the black 10Hz trace developed. The appearance of higher frequencies on the black 10Hz trace, such as the asymmetry on the leading edge of the sine wave and the bump on the trailing edge, are indications of the development of small cracks on the sample. Prior to this time, both the 5Hz and 10Hz signals appeared to be pure sine waves. Also, after this observation, the sample's surface was abraded and cleaned with fiberglass "Scotch-brite." After this cleaning, the 10Hz signal (side lobe on the descending edge of the 5Hz signal in the black trace) disappeared, apparently due to the removal of the micro cracks developed during the previous stress cycles. This also points to the validity of the "blending" process used to remove small visible cracks in the surface of turbine engine blades.

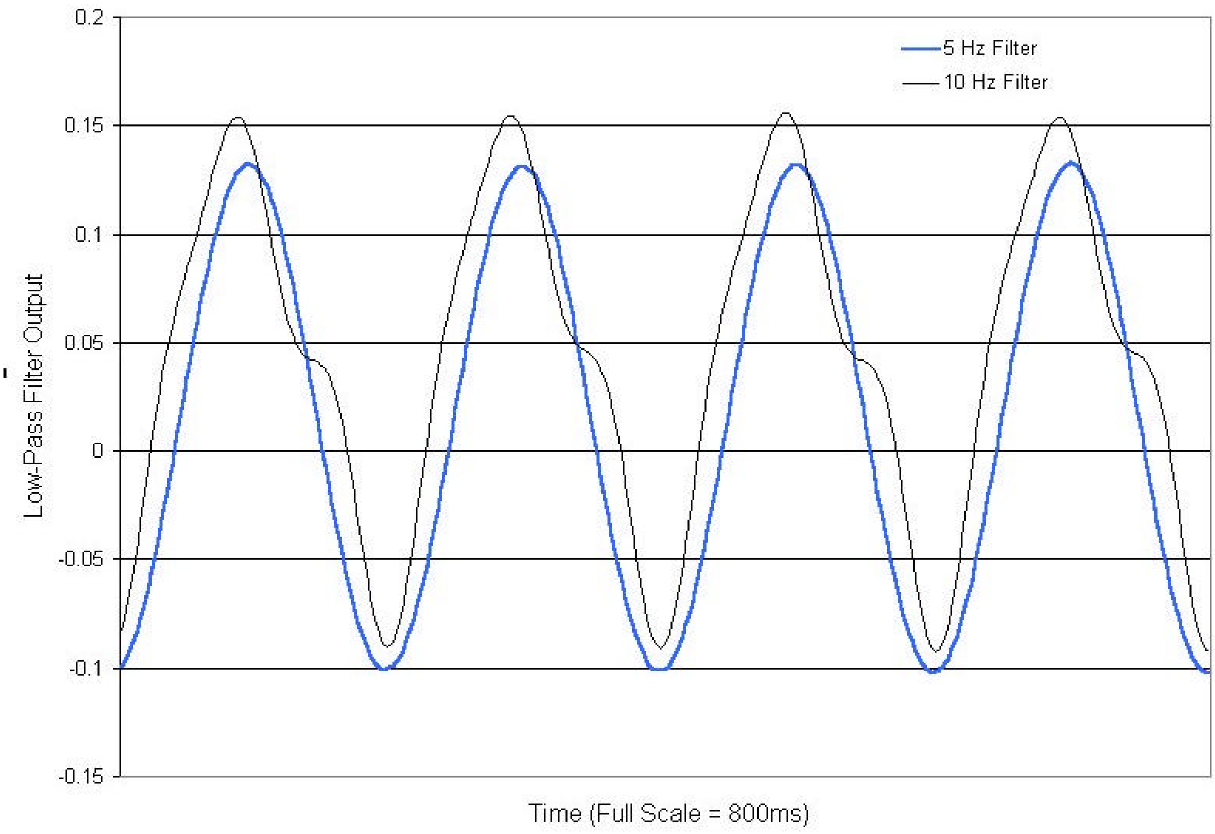

Figure 7. 5Hz and 10Hz Filtered EFS Signals

3.0 Ultrasonic Inspection

A portable, battery operated, Staveley Sonic 1200 HR ultrasonic electronics unit was coupled to the ultrasonic transducer (UT) probes to provide the pulsed signal to the transducer, collect the reflected pulses, and analyze and present the data. Two different types of UT probes were constructed: a shear wave (delay line) and a surface wave.

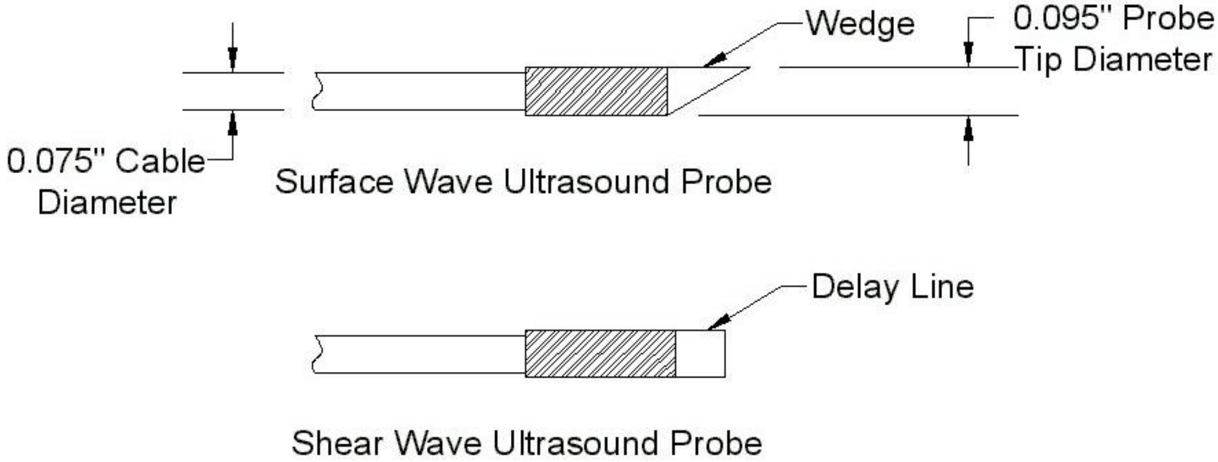

Figure 8. Ultrasound Probes

The delay line probe was used for checking the thickness of sample material, and had a thickness measurement range of 0.25 - 4.5mm. The transducer has an operating frequency of 10 MHz with a crystal diameter of 2.0mm. The tip of the probe measured 2.4mm diameter X 7.6mm long, and was made as small as reasonably possible in order to be able to transverse the 3mm working channel within the borescope, yet retain enough transducer area to produce signals with reasonable S/N.

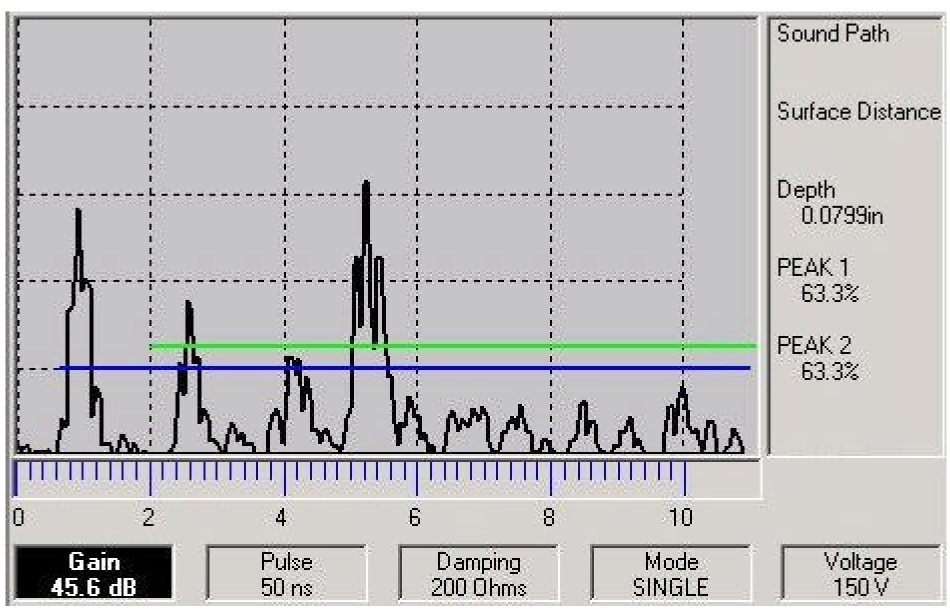

Figure 9. Delay Line Ultrasonic Display of 0.080” Thick Test Plate

The surface wave probe retained many of the characteristics of the delay line, both dimensionally and in operating frequency. The angled Lucite wedge at the front of the transducer provided more controllable surface contact than the delay line, making it easier to use for the operator. Also, the surface wave system permitted the detection of surface-breaking defects such as voids or cracks.

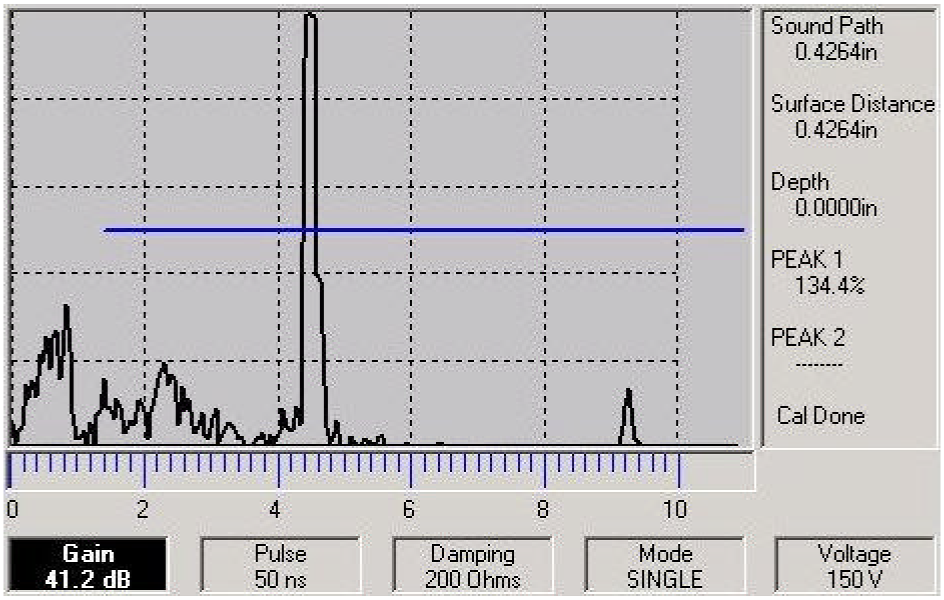

Figure 10. Surface Wave Ultrasonic Signal of Distant Crack
(Crack is 0.43" From Sensor)

4.0 Eddy Current Inspection

A portable, battery operated, Staveley Nortec 2000S electronics unit was used or collecting and processing the eddy current probe data. First attempts at relative probes proved to be too sensitive to lift-off from the sample, and difficult to reduce in size to the required dimensions for passing through the working channel. We finalized on a miniature pencil probe with an absolute wound coil for the detection of surface breaking defects. The coil operated at a frequency of 1 MHz and had an outside diameter of 2.5mm. The absolute coil is unshielded, so that the sides of the probe can be used for scanning without concern for the probe’s axial position with respect to the sample.

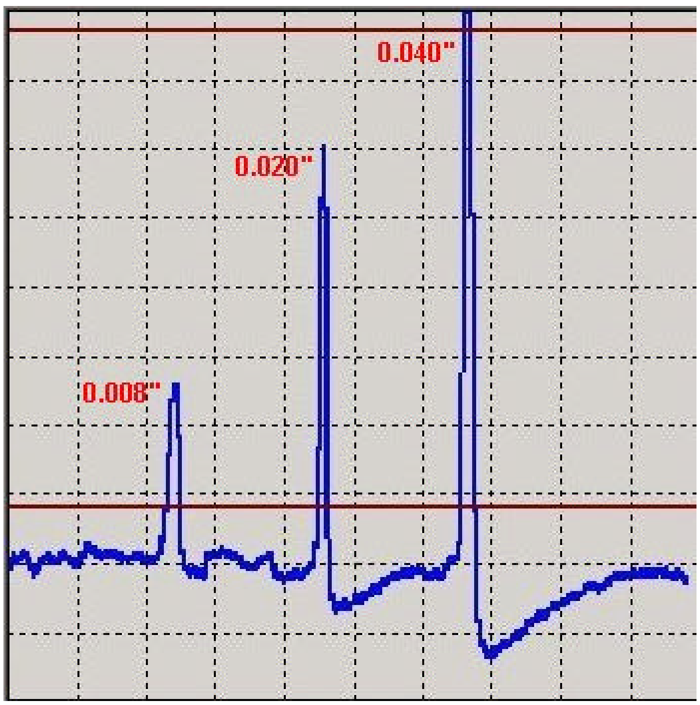

Figure 11. Absolute Eddy Current Signals from 0.005” Wide Cracks of Various Depths

5.0 Borescope Delivery System

Current borescope technology is unsuitable for fully interrogating components within an aircraft engine without disassembling the engine. The main focus of this investigation was to improve upon existing technology to produce a borescope engine inspection system that could:

- visually inspect the interior of an engine
- deliver ultrasonic probes within the engine
- deliver eddy current probes within the engine
- deliver EFS within an engine
- articulate 90° around a hemisphere at the distal end of the borescope
- provide an intuitive operator interface to articulation of the borescope
- maintain a borescope outer diameter of no more than 6mm

While working with the various probes configured for the borescope, it became apparent that several changes needed to be made to the design of the scope. Most apparent was the need for a different articulation mechanism than the traditional "two knob" system. The need arose because of the scanning requirements of the probes, particularly the eddy current probe. This probe requires that it be scanned over a crack in order to detect it. Scanning with the two-knob articulation mechanism required an extremely skilled operator and/or two hands on the scope handle/knobs. The operator would, therefore, need to release the scope shaft in order to operate the borescope's articulation mechanism. This was unsatisfactory because both the eddy current and the ultrasonic probes are sensitive to lift off of the probe tip from the sample. We abandoned the original articulation design and modified an intuitive articulation mechanism that we developed for medical applications.

The current borescope design expands the scope's ability to articulate, from the original 2-way articulation, where the distal tip had a range of ±70° in only one plane, to Allway™ articulation whereby the scope's tip can be pointed in any direction within a 90 degree hemisphere. This required the use of two sets of push/pull wires to accomplish articulation, but the typical two-knob articulation system was too cumbersome and difficult to use. The counterintuitive nature of the two-knob articulation mechanism was overcome by the implementation of a mechanical joystick. The joystick's movement is intuitive, and directly relates to the direction of movement of the distal end of the borescope. The joystick can be operated with only one hand, thereby freeing the other hand to manipulate or support the scope shaft, or move probes and tools through the working channel. And, unlike an electronic servomotor driven joystick, a mechanical joystick is: more robust, simple, lighter, and it provides direct tactile feedback to the operator of any resistance that the scope's tip is experiencing. Therefore, the operator is much less likely to overshoot the articulation mechanism, which could result in damage to the item being inspected, and damage to the borescope articulation mechanism and/or vertebrae.

Moving to the mechanical joystick, because of its intuitive nature and tactile feedback, also created unexpected problems with the way in which the original borescope was designed. There is a limited range of comfortable travel for a typical operator's thumb of approximately ±30°. However, the borescope's end tip must articulate 90° in all directions. Since there is a minimum amount of torque required to articulate the scope, and a maximum amount of force a typical operator can comfortably exert on the joystick, a reexamination of torque, forces, gear ratios, and material selection had to be undertaken in order to make the joystick not only operable, but also comfortable to operate.

In order to reduce the amount of force required to articulate the borescope, several changes were made to the construction of the scope's insertion tube. The outer tungsten braid wire diameter was reduced slightly in order to minimize its stiffness while retaining its mechanical wear characteristics in protecting the scope from accidental damage. Along with this reduction the braid was manufactured on a smaller core than the shaft assembly. This forced the braid to be compressed over the vertebrae section thus creating a spring like characteristic that aids the vertebrae while articulating. The light guide were changed from 0.5mm diameter plastic fiber to bundles of 30μm diameter glass fibers, again to improve flexibility and cut down on the amount of force required to bend the end of the scope. One of the biggest challenges, and largest contributors to the scope's stiffness, was the working channel material. This channel must be able to smoothly and easily pass the various probes used to interrogate the sample, while at the same time be flexible and not kink when bent. We finalized on a thin-wall flexible PVC laminate in which a monocoil (spring) was embedded between two layers of elastomer. This provided the hoop strength to the channel material that prevented its collapse while bending, yet gave it enough flexibility so as not to add substantially to the stiffness of the shaft.

Yet another change for the final borescope design was the modification of the articulation vertebrae. The original vertebrae was designed for two-way articulation in a single plane of operation. While we have a 8mm diameter Allway™ vertebrae constructed of plastic links, the diameter of this vertebrae was too large for the current application, and it could not be scaled down in size to meet the 6mm maximum requirement for engine inspection. A new 6mm vertebrae was designed, with extremely thin walls, capable of articulating within a 90° hemisphere, and possessing a bend radius of 25mm. These changes were necessary in order to reduce the bending radius of the articulation section, which is critical in accessing tight spaces within an engine and for proper placement of the probes.

Figure 12. Articulation Link Pair.

The final vertebrae links were manufactured using EDM and grinding processes. This permitted the links to be manufactured from stainless steel, allowing wall thickness as low as 0.1mm, yielding more space for the working channel and other borescope internal components. This increase in interior area within the vertebrae also helped reduce the stiffness of the distal end of the shaft, further reducing the force required to articulate the shaft.

The above changes to the shaft components permitted the joystick mechanism to overcome the force and torque requirements needed to properly articulate the distal end of the scope. Additionally, these changes allowed the shaft length to increase, the bend radius to decrease, and sufficient space to permit the ultrasonic, eddy current, and EFS probes to be delivered through the borescope to a remote location.

Borescope Specifications

<u>Mechanical Properties:</u>	
Outer Diameter	6mm
Working Length	1.5m
Working Channel Inside Diameter	3mm
Articulation	90° AllWay™ Articulation
Minimum Bend Radius	25mm
Shaft Covering	Braided Tungsten over Urethane
Operating Temperature	0-54°C
Handle	Custom SLA
Storage Case	Gray Pelican
<u>Optical Properties:</u>	
Dept of Field	5-50mm
Field of View	50°
Resolution	2 lp/mm at 5mm
Image Bundle	0.4mm diameter Quartz 6,000 pixels
Video Direct Imager	1/3" Color CCD 410,000 pixels 768 (H) x 494 (V) Video Resolution
Light Guide	Detachable Glass, ACMI Connector
Light Source	MS-48 Portable/Rechargeable 12V, 2A Metal Halide 5460 Color Temperature Rechargeable Li-Ion Battery / 115VAC

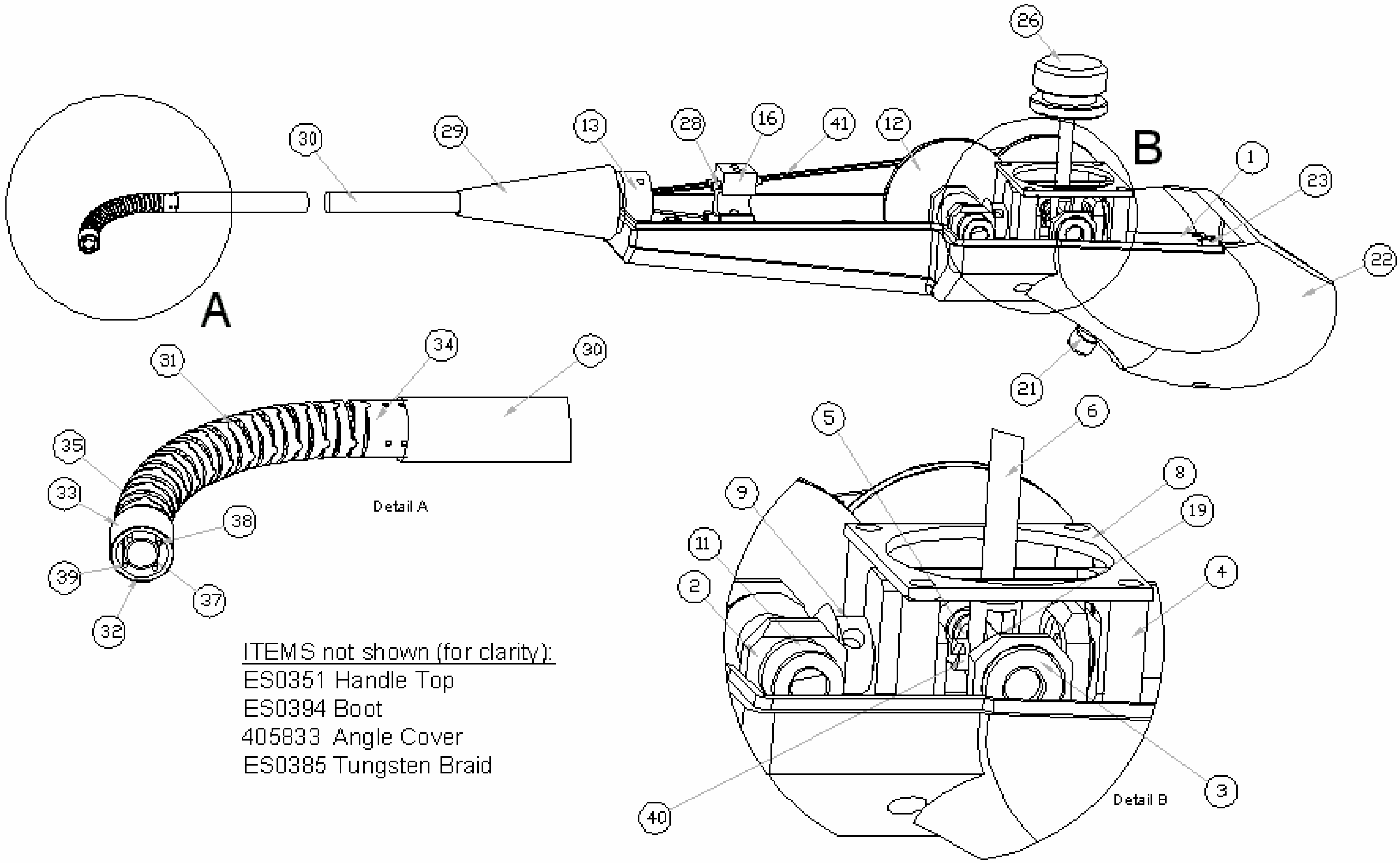

Figure 13. Borescope Assembly

Borescope Assembly Bill of Material

Item #	Part #	Description
1	ES0347	BASE PLATE
2	ES0337	BEARING BLOCK
3	ES0310	BEARING
4	ES0392	STANDOFF
5	ES0335	PULLY ARM
6	ES0336	ARM COUPLER
7	ES0338	ARC GUIDE
8	ES0346	STOP PLATE
9	ES0339	GEAR MODIFIED
10	ES0340	SHAFT LONG
11	ES0302	SHAFT COLLAR
12	ES0300	DRUM
13	ES0124	SHAFT COUPLER
14	ES0027	CAMERA
15	ES0107	CAMERA BLOCK
16	ES0348	SPRING GUIDE BLOCK
17	ES0367	LUER FITTING MOD
18	ES0341	SHAFT SHORT
19	ES0390	WASHER TEFLON
20	ES0344	SHAFT SPACER
21	ES0397	ACMI CONNECTOR
22	ES0350	HANDLE BOTTOM

23	ES0393	SPACER
24	ES0387	GROMMET
25	ES0343	ACMI MOUNT
26	ES0349	JOYSTICK CAP
27	ES0342	SHAFT MID
28	ES0398	SPRING GUIDE STOP
29	405787	STRAIN RELIEF
30	ES0404	MASTER SHEATHING
31	004871	VERTEBRAE LINK
32	ES0361	HEAD DISTAL
33	ES0360	SLEEVE HEAD
34	ES0362	SPRING GUIDE COLLAR
35	ES0401	VERTIBREA LINK MOD
36	ES0372	SPRING GUIDE SLEEVE
37	ES0384	WORKING CHANNEL
38	ES0395	QUARTZ IMAGE GUIDE
39	012045	LIGHT GUIDE FIBER
40	ES0391	COUPLER SCREW
41	409048	CONTROL WIRE
42	ES0351	HANDLE TOP
43	ES0394	BOOT
44	405833	ANGLE COVER
45	ES0385	BRAID TUNGSTEN

6.0 Conclusions

Improvements to current borescope design, including a more intuitive articulation mechanism and the development of a 6mm diameter borescope with a 3mm diameter working channel, permit the delivery of visual, ultrasonic, eddy current, and EFS probes to internal components of aircraft engine. Current technologies that produce sufficient force to result in EFS signals, however, are too large to be delivered within the 6mm diameter access to the engine. Nonetheless, the ability to visually inspect engine components, and then verify the presence or absence of cracks with eddy current or ultrasonic probes, is a valuable tool for the nondestructive testing of aircraft fatigue critical locations.

Future work should incorporate all system components (borescope, light source, video display, computer, eddy current and ultrasonic electronics, and EFS) into a single, portable instrument. An effort is also needed to produce user-friendly software to operate the instrumentation, and to integrate the data from the various sensors into a single database. More ergonomic design work is also necessary for the joystick handle.

Also needed for EFS to function within an on-wing aircraft engine is a mechanism to apply the necessary load for the production of an EFS signal. Currently, the technology is not available to apply the necessary load within the tight confines of an engine. In future engine designs, this mechanism, or an access port for the mechanism, could be designed into the engine.

Appendix A: Borescope Detail Drawing List

FILE NAME	SIZE	FILE TYPE
2100r0 (NECP-1010-R1) EDDY PROBE.PDF	19KB	Adobe Acrobat Document
ES0020 MONOCOIL.DWG	61KB	AutoCAD Drawing
ES0021 SHEATHING.DWG	55KB	AutoCAD Drawing
ES0024 SPRING GUIDE.DWG	55KB	AutoCAD Drawing
ES0027 CAMERA.DWG	55KB	AutoCAD Drawing
ES0027 CAMERA.SLDPRT	53KB	SLDPRT File
ES0063 COUPLER HOUSING.DWG	60KB	AutoCAD Drawing
ES0064 LENS BARREL.DWG	49KB	AutoCAD Drawing
ES0070 NUT.DWG	44KB	AutoCAD Drawing
ES0079 LENS.DWG	44KB	AutoCAD Drawing
ES0080 LENS ASSEMBLY.DWG	41KB	AutoCAD Drawing
ES0083 LUER FITTING.DWG	44KB	AutoCAD Drawing
ES0107 CAMERA BASE.DWG	51KB	AutoCAD Drawing
ES0107 CAMERA BLOCK.SLDPRT	92KB	SLDPRT File
ES0124 SHAFT COUPLER.DWG	59KB	AutoCAD Drawing
ES0124 SHAFT COUPLER.SLDPRT	103KB	SLDPRT File
ES0300 DRUM.DWG	60KB	AutoCAD Drawing
ES0300 DRUM.SLDPRT	118KB	SLDPRT File
ES0301 GEAR.DWG	58KB	AutoCAD Drawing
ES0302 COLLAR.DWG	56KB	AutoCAD Drawing
ES0302 SHAFT COLLAR.SLDPRT	202KB	SLDPRT File
ES0310 BEARING.DWG	59KB	AutoCAD Drawing
ES0310 BEARING.SLDPRT	116KB	SLDPRT File
ES0335 PULLY ARM.SLDDRW	328KB	SLDDRW File
ES0335 PULLY ARM.SLDPRT	123KB	SLDPRT File
ES0336 ARM COUPLER.SLDDRW	332KB	SLDDRW File
ES0336 ARM COUPLER.SLDPRT	167KB	SLDPRT File
ES0337 BEARING BLOCK.SLDDRW	285KB	SLDDRW File
ES0337 BEARING BLOCK.SLDPRT	119KB	SLDPRT File
ES0338 ARC GUIDE.SLDDRW	325KB	SLDDRW File
ES0338 ARC GUIDE.SLDPRT	205KB	SLDPRT File
ES0339 GEAR MODIFIED.SLDDRW	292KB	SLDDRW File
ES0339 GEAR MODIFIED.SLDPRT	122KB	SLDPRT File
ES0340 SHAFT LONG.SLDDRW	268KB	SLDDRW File
ES0340 SHAFT LONG.SLDPRT	94KB	SLDPRT File
ES0341 SHAFT SHORT.SLDDRW	293KB	SLDDRW File
ES0341 SHAFT SHORT.SLDPRT	88KB	SLDPRT File
ES0342 SHAFT MID.SLDDRW	294KB	SLDDRW File
ES0342 SHAFT MID.SLDPRT	76KB	SLDPRT File
ES0343 ACMI MOUNT.SLDDRW	324KB	SLDDRW File

Appendix A: Borescope Detail Drawing List
continued

FILE NAME	SIZE	FILE TYPE
ES0343 ACMI MOUNT.SLDPRT	104KB	SLDPRT File
ES0344 SHAFT SPACER.SLDDRW	286KB	SLDDRW File
ES0344 SHAFT SPACER.SLDPRT	82KB	SLDPRT File
ES0346 STOP PLATE.SLDDRW	333KB	SLDDRW File
ES0346 STOP PLATE.SLDPRT	110KB	SLDPRT File
ES0347 BASE PLATE HOLE DIM.SLDDRW	633KB	SLDDRW File
ES0347 BASE PLATE.SLDDRW	597KB	SLDDRW File
ES0347 BASE PLATE.SLDPRT	452KB	SLDPRT File
ES0348 SPRING GUIDE BLOCK.SLDDRW	454KB	SLDDRW File
ES0348 SPRING GUIDE BLOCK.SLDPRT	292KB	SLDPRT File
ES0349 JOYSTICK CAP.SLDDRW	325KB	SLDDRW File
ES0349 JOYSTICK CAP.SLDPRT	86KB	SLDPRT File
ES0350 HANDLE BOTTOM.SLDDRW	550KB	SLDDRW File
ES0350 HANDLE BOTTOM.SLDPRT	1,166KB	SLDPRT File
ES0351 HANDLE TOP.SLDDRW	228KB	SLDDRW File
ES0351 HANDLE TOP.SLDPRT	744KB	SLDPRT File
ES0360 SLEEVE HEAD.SLDDRW	140KB	SLDDRW File
ES0360 SLEEVE HEAD.SLDPRT	73KB	SLDPRT File
ES0361 HEAD DISTAL.SLDDRW	299KB	SLDDRW File
ES0361 HEAD DISTAL.SLDPRT	196KB	SLDPRT File
ES0362 SPRING GUIDE COLLAR.SLDDRW	352KB	SLDDRW File
ES0362 SPRING GUIDE COLLAR.SLDPRT	219KB	SLDPRT File
ES0367 LUER FITTING MOD.SLDPRT	84KB	SLDPRT File
ES0368 MASTER SHEATHING.DWG	123KB	AutoCAD Drawing
ES0368 MASTER SHEATHING.SLDPRT	55KB	SLDPRT File
ES0372 SPRING GUIDE SLEEVE.SLDDRW	287KB	SLDDRW File
ES0372 SPRING GUIDE SLEEVE.SLDPRT	68KB	SLDPRT File
ES0384 WORKING CHANNEL.SLDPRT	35KB	SLDPRT File
ES0385 BRAID.DWG	85KB	AutoCAD Drawing
ES0387 GROMMET.SLDDRW	132KB	SLDDRW File
ES0387 GROMMET.SLDPRT	85KB	SLDPRT File
ES0388 SPRING WASHER.SLDDRW	132KB	SLDDRW File
ES0390 WASHER TEFLON.SLDPRT	28KB	SLDPRT File
ES0391 COUPLER SCREW.SLDDRW	278KB	SLDDRW File
ES0391 COUPLER SCREW.SLDPRT	99KB	SLDPRT File
ES0391 WASHER TEFLON.SLDDRW	133KB	SLDDRW File
ES0392 STANDOFF.SLDDRW	269KB	SLDDRW File
ES0392 STANDOFF.SLDPRT	56KB	SLDPRT File
ES0393 SPACER.SLDDRW	266KB	SLDDRW File

Appendix A: Borescope Detail Drawing List
continued

FILE NAME	SIZE	FILE TYPE
ES0393 SPACER.SLDPRT	59KB	SLDPRT File
ES0394 BOOT.SLDPRT	326KB	SLDPRT File
ES0395 QUARTZ IMAGE GUIDE LENSED.DWG	57KB	AutoCAD Drawing
ES0395 QUARTZ IMAGE GUIDE.SLDPRT	33KB	SLDPRT File
ES0396 SCOPE ASSEMBLY.SLDASM	1,805KB	SLDASM File
ES0396 SCOPE ASSEMBLY.SLDDRW	827KB	SLDDRW File
ES0397 ACMI CONNECTOR.DWG	70KB	AutoCAD Drawing
ES0397 ACMI CONNECTOR.SLDPRT	166KB	SLDPRT File
ES0398 SPRING GUIDE STOP.SLDDRW	275KB	SLDDRW File
ES0398 SPRING GUIDE STOP.SLDPRT	40KB	SLDPRT File
ES0399 HANDLE ASSEMBLY.SLDDRW	115KB	SLDDRW File
ES0400 DISTAL ASSEMBLY.SLDASM	595KB	SLDASM File
ES0401 VERTIBREA LINK MOD.SLDPRT	246KB	SLDPRT File
ES0402 QUARTZ BUNDLE HOLDER.SLDDRW	365KB	SLDDRW File
ES0402 QUARTZ BUNDLE HOLDER.SLDPRT	89KB	SLDPRT File
ES0403 COUPLER HOUSING.DWG	66KB	AutoCAD Drawing
ES0405 SHAFT SLEEVE.SLDDRW	109KB	SLDDRW File
ES0405 SHAFT SLEEVE.SLDPRT	36KB	SLDPRT File
ES0406 FERRULE FOR IMAGE BUNDLE.SLDDRW	130KB	SLDDRW File
ES0406 FERRULE FOR IMAGE BUNDLE.SLDPRT	34KB	SLDPRT File
ES0409 COUPLING DELIVERY SYSTEM.SLDDRW	115KB	SLDDRW File
ES0410 EFS WIRING HARNESS	353KB	SLDDRW File
ES0411 BNC T	299KB	SLDDRW File
004871 VERTEBRAE LINK.SLDPRT	343KB	SLDPRT File
004871 VERTIBREA LINK ASSEMBLY.SLDASM	174KB	SLDASM File
004871 VERTEBREA LINK REV 8.DWG	100KB	AutoCAD Drawing
012045 LIGHT GUIDE FIBER.SLDPRT	32KB	SLDPRT File
405787 STRAIN RELIEF.DWG	53KB	AutoCAD Drawing
405787 STRAIN RELIEF.SLDPRT	85KB	SLDPRT File
409048 CONTROL WIRE.SLDPRT	34KB	SLDPRT File
CX227A UT DELAY PROBE.DWG	18KB	AutoCAD Drawing
CX228A UT SURFACE PROBE.DWG	21KB	AutoCAD Drawing
ORENTATION BLOCK.SLDPRT (for reference only)	106KB	SLDPRT File
TEMPLATE.SLDDRW (for reference only)	227KB	SLDDRW File

Appendix B: EFS Electronics Settings

- AMEL 2059 Potentiostat
  - +0.455V Grounded Operation
  - Working Electrode and Sample connected to ground
  - Counter and Reference Electrode connected to EFS Electrode
  - Potential Current Potentiostat = 0.1
  - Backing Off = Off
  - IR Compression = Off
  - V(out) = Off
  - Function = Potentiostat (button in)
  - Polarity = + (button in)

- SR640 Dual Channel Low-Pass Filter
  - CHANNEL 1:
    - AC Coupled
    - 6 Hz
    - Gain (input) = 20dB
    - Gain (output) = 0dB
  - CHANNEL 2:
    - AC Coupled
    - 16 Hz
    - Gain (input) = 30dB
    - Gain (output) = 10dB

- SR803 Lock-In Amplifier #1 – 10 Hz Signal
  - τ = 10s
  - Sensitivity = 50mV
  - Signal Input = A
  - Reserve = Normal
  - Filters = Line
  - CH1 Output = X
  - CH2 Output = θ
  - Harmonic = 2
  - Frequency Reference Input from Lock-In #2 @ 5Hz

- SR803 Lock-In Amplifier #2 – 5Hz
  - τ = 10s
  - Sensitivity = 50mV
  - Signal Input = A
  - Reserve = Normal
  - Filters = Line
  - CH1 Output = X
  - CH2 Output = θ
  - Amplitude = 0.150V
  - Reference Frequency = 5.000Hz

- PCI-DAS 1602-16 16 Channel A/D
  - Input Voltage Range = ±10V
  - Channel Assignments:
    - Ch1 – 5Hz Reference
    - Ch2 – Potentiostat Output
    - Ch3 – 5Hz Lock-In X
    - Ch4 – 5Hz Lock-In θ
    - Ch5 – 10Hz Lock-In X
    - Ch6 – 10Hz Lock-In θ
    - Ch7 – 5Hz Low-Pass Filter Output
    - Ch8 – 10Hz Low-Pass Filter Output

- KEPCO BOP 20-10M Op-Amp
  - Reference Input = 5Hz Sine Wave from 5Hz Lock-In Reference Output
  - External Resistor (Back Panel) = 59KΩ (fixed) in parallel with 50KΩ Pot.
  - Minimum Load Settings:
    - Force = 4 pounds
    - Output Current = 1.6A
    - Output Voltage = 3.52V
  - Maximum Load Settings:
    - Force = 15 pounds
    - Output Current = 6.0A
    - Output Voltage = 13.2V

Appendix C: Eddy Current Probe Standard Programs

	Steel	Aluminum
Frequency	1.0 MHz	1.0 MHz
H-Gain	69.1 dB	62.8 dB
V-Gain	69.1 dB	82.8 dB
Angle	240.3	249.1
H-Position	50.0%	50.0%
V-Position	30.0%	30.0%
LP Filter	100	100
HP Filter	Off	Off
Sweep	1.000s	1.000s
Cont Null	1.0 Hz	1.0 Hz
Prove Driv	Mid	Mid
Sweep Erase	On	On
Dot/Box	Box	Box
Horn	Off	Off
Capture	2.5 s	5.0 s
Disp Ers	Off	Off
Graticule	On	On
Persist	Off	Off
Alarm	Sweep	Sweep
Alarm Dwell	0	0
Sweep	Off	Negative
Top	75.0%	72.0%
Bottom	25.0%	3.0%

Appendix D: Ultrasonic Probe Standard Programs

	Surface Wave Probe	Shear Wave No Delay	Shear Wave Delay
PULSER			
Pulser	50 ns	50 ns	50 ns
Damping	200	200	200
Mode	Single	Single	Single
Voltage	150 V	150 V	150 V
RECEIVER			
Gain	41.2 dB	72.4 dB	52.6 dB
Display	Fullwave	Fullwave	Fullwave
Frequency	10 MHz	10 MHz	10 MHz
Reject	0%	0%	0%
DB Diff	0 dB	0 dB	0 dB
GATE			
Gate 1	+	+	+
Level	44%	50%	31%
Position	0.439 in	0.173 in	0.318 in
Width	2.0 in	1.000 in	1.000 in
Gate 2	Off	+	+
Level	50%	58%	35%
Position	0.500 in	0.070 in	0.029 in
Width	0.250 in	1.000 in	1.000 in
RANGE			
Range	1.000 in	1.000 in	0.250 in
Delay	0.284 in	0.000 I	0.262 in
Vel	0.1260	0.2310	0.2310
Rep Rate	150 Hz	2000 Hz	2000 Hz
DAC	Off	Off	Off

Appendix D: Ultrasonic Probe Standard Programs
continued

	Surface Wave Probe	Shear Wave No Delay	Shear Wave Delay
SPCL			
Units	in	in	in
+dB Val	6.0 dB	6.0 dB	6.0 dB
Peakhold	Off	Off	Off
THICKNESS			
T-Gauge	IP-1st	Auto E-E	Auto E-E
Trigger	Edge	Edge	Edge
Offset	6.475 us	0.000 us	0.000 us
T-Vel	0.2432	0.2310	0.2310
Trip	Off	Off	Off
Angle	90.0	90.0	0
Thick	0.0973	0.0996 in	0.0996 in
O-Diam	Off	Off	Off